Research Square

Preprints are preliminary reports that have not undergone peer review.
They should not be considered conclusive, used to inform clinical practice,
or referenced by the media as validated information.

# Brain Tissue Proportionality and General Cognitive Ability Across Three Adult Cohorts

**Baptiste Dumoulin**

baptiste.dumoulin@chu-brugmann.be

CHU Brugmann University Hospital

**Research Article**

**Keywords:** general cognitive ability, brain structure, cerebellum, white matter, compositional data analysis, structural MRI

**Posted Date:** November 2nd, 2026

**DOI:** https://doi.org/10.21203/rs.3.rs-11527260/v1

**License:** This work is licensed under a Creative Commons Attribution 4.0 International License.
Read Full License

**Additional Declarations:** No competing interests reported.

# Brain Tissue Proportionality and General Cognitive Ability Across Three Adult Cohorts

**Baptiste Dumoulin, MSc**

Clinical Research Unit, CHU Brugmann University Hospital, Brussels, Belgium

Corresponding author: Baptiste Dumoulin | baptiste.dumoulin@chu-brugmann.be

ORCID: 0009-0002-0062-9151

## Article information

Research paper | Brain Structure and Function

Short title: Brain tissue proportionality and cognition

Abstract: 194 words. Main prose: 3,713 words excluding abstract, headings, declarations, references, tables and captions.

Three main tables and three main figures. Online Resource 1: supplementary methods, Tables S1–S12 and Fig. S1. Online Resource 2: Supplementary Code 1.

## Acknowledgements

Data were provided in part by the Human Connectome Project, WU-Minn Consortium (Principal Investigators: David Van Essen and Kamil Ugurbil; 1U54MH091657) funded by the 16 NIH Institutes and Centers that support the NIH Blueprint for Neuroscience Research; and by the McDonnell Center for Systems Neuroscience at Washington University. The author also thanks the investigators and participants of the Dallas Lifespan Brain Study and the Amsterdam Open MRI Collection.

## Abstract

General cognitive ability may relate to the proportional allocation of brain tissue beyond overall tissue volume. We examined five FreeSurfer compartments using compositional data analysis: cortical gray matter, cerebral white matter, subcortical gray matter, total cerebellum, and brainstem. Human Connectome Project Young Adult data (HCP-YA; N = 1,101) provided discovery estimates; the Dallas Lifespan Brain Study (DLBS; N = 418) and Amsterdam Open MRI Collection ID1000 (AOMIC; N = 926) provided independent cohort tests. Four isometric log-ratio coordinates represented composition, with age, sex, and log total analyzed tissue volume included separately. Composition explained additional cognitive variance in DLBS (partial $R^2$ = 4.20%, p = .00154) and AOMIC (partial $R^2$ = 1.35%, p = .014). The total-cerebellum-to-cerebral-white-matter contrast selected in HCP was positive in both replication cohorts: standardized $\beta = 0.162$ (heteroskedasticity-robust 95% confidence interval 0.072–0.252) in DLBS and 0.097 (0.024–0.170) in AOMIC. Participant-pairs bootstrap intervals supported both associations. Replacing total tissue volume with estimated intracranial volume attenuated the AOMIC association, whereas including both preserved it. Relative macroanatomical allocation is associated with broad cognitive ability conditional on analyzed tissue volume, with differing effect magnitudes across cohorts. These cross-sectional findings do not establish causal tissue trade-offs.

Keywords: general cognitive ability; brain structure; cerebellum; white matter; compositional data analysis; structural MRI

## 1 Introduction

General cognitive ability (g) summarizes shared variation across diverse cognitive tasks. Neuroimaging studies have examined its regional and whole-brain correlates (Jung and Haier 2007; Deary et al. 2010; Dubois et al. 2018; Wilcox et al. 2026). A meta-analysis of 148 samples found a modest positive brain-volume–intelligence association, with estimated magnitudes affected by study quality and reporting bias (Pietschnig et al. 2015).

Overall size leaves a different anatomical question unresolved: individuals with similar total tissue volume can differ in its allocation among cortical gray matter, cerebral white matter, subcortical gray matter, cerebellum and brainstem. Log-ratios represent these relative amounts jointly, respecting their dependence at a fixed total. This rationale does not make regressions on unclosed raw volumes intrinsically invalid.

Compositional data analysis (CoDA) represents relative measurements through log-ratios (Aitchison 1986). Isometric log-ratio (ILR) coordinates map a D-part composition onto $D-1$ orthonormal coordinates (Egozcue et al. 2003). Compositional brain scores have distinguished Alzheimer-related volumetric patterns (Genius et al. 2025). We apply this framework to cognition and the relative allocation of five major tissue compartments.

Cerebellar volumes have been associated with cognitive outcomes, sometimes attenuating after overall-size adjustment (Andreasen et al. 1993; Paradiso et al. 1997; Hoogendam et al. 2014). Cerebellar territories also map to cerebral association networks (Buckner et al. 2011). Complementing regional gray-matter prediction studies (Hilger et al. 2020), we ask whether major-compartment configuration relates to g beyond the summed volume of those compartments.

The Human Connectome Project Young Adult cohort (HCP-YA) provided discovery data. Its selected total-cerebellum-to-cerebral-white-matter balance was then specified for the independent Dallas Lifespan Brain Study (DLBS) and retained for additional replication in Amsterdam Open MRI Collection (AOMIC) ID1000. This sequence examines generalization across cognitive batteries, ages and imaging pipelines (Fig. 1).

## 2 Methods

### 2.1 Study design and analysis sequence

This secondary analysis proceeded from HCP-YA discovery to DLBS confirmation and AOMIC additional replication. The global composition and ten pairwise balances were examined in HCP. The five-part representation, global test and selected focal contrast were retained in DLBS and AOMIC. The primary AOMIC model and original sensitivities were specified before its association testing; this internal specification accompanies the code (Online Resource 2), but was not publicly preregistered. Later domain, pairwise, tissue-decomposition and synthesis analyses are exploratory.

The outcome was a standardized first principal component (PC1) from each cohort's multidomain cognitive battery. Anatomical exposures were the five compartments, with their sum modeled separately as total analyzed tissue volume. Cohorts were analyzed separately without assuming identical cognitive measurement or effect magnitude.

### 2.2 Human Connectome Project Young Adult cohort

HCP-YA data were obtained from the 2025 release of the WU–Minn Human Connectome Project through ConnectomeDB powered by BALSA (Human Connectome Project 2025; Van Essen et al. 2013). The public export contained 1,206 participant records. Complete data on all prespecified cognitive tests, demographic covariates, intracranial volume, and the eight FreeSurfer variables required to construct the five anatomical compartments were available for 1,101 participants. The complete-case sample included 596 women and 505 men. HCP age was available in public age bands: 22–25 years (n = 230), 26–30 (n = 482), 31–35 (n = 377), and 36+ (n = 12).

The ten HCP tests covered vocabulary, reading, reasoning, spatial orientation, episodic and working memory, executive control, attention and processing speed (Table S1; Dubois et al. 2018; Wilcox et al. 2026). Tests were z-standardized before PCA, and PC1 was standardized to mean zero and SD one.

HCP-YA includes twins and siblings. Family identifiers were unavailable, so full-sample HCP estimates are used for discovery and their reported uncertainty is nominal, without adjustment for family dependence. Confirmatory tests use DLBS and AOMIC as specified below.

### 2.3 Dallas Lifespan Brain Study

DLBS is an open longitudinal study of adult brain and cognitive aging. Its published baseline sample comprised 464 adults aged 21–89 years (Park et al. 2025). Data were obtained from OpenNeuro ds004856, version 1.3.0, and only Wave 1 was analyzed. Complete cognitive and structural data were available for 418 participants (260 women, 158 men). The available age-band midpoints ranged from 21 to 90 years (mean 58.2, SD 18.3); these are modeled midpoints, not exact individual ages. Mean estimated education was 15.7 years (SD 2.2), and mean Mini-Mental State Examination score was 28.4 (SD 1.2).

DLBS cognitive inputs were processing speed, working memory, reasoning, vocabulary and verbal fluency. Selected task totals were oriented toward better performance, standardized across Wave 1 and averaged within domains. The five domain composites were standardized before PCA; PC1 was then standardized as g. Task selection and scoring are detailed in Online Resource 1, and PC1 weights appear in Table S1.

### 2.4 Amsterdam Open MRI Collection

AOMIC ID1000 released 928 participants aged 19–26, recruited to represent Dutch educational levels (Snoek et al. 2021). Participant and FreeSurfer tables from OpenNeuro ds003097 v1.2.1 were matched one-to-one at a fixed repository commit. Eligibility required finite age, sex category, complete cognitive domains and positive finite anatomical volumes. Two participants lacked cognitive scores, leaving 926 (481 female; mean age 22.85, SD 1.71). Primary exclusions were not outcome-based. Genetic unrelatedness was not independently verified.

AOMIC PC1 used standardized Intelligence Structure Test domains: fluid intelligence, memory and crystallized intelligence. Weights were oriented to sum positively; PC1 was standardized to population SD one. The redundant native total was reserved as an alternative outcome. Analyses used released FreeSurfer 6.0.1 summaries; source versions, scoring and checksums accompany the code.

### 2.5 Anatomical representation

Structural variables were derived using FreeSurfer, retaining each cohort's acquisition and processing pipeline (Dale et al. 1999; Fischl et al. 2002; Fischl 2012). The five parts were total cortical gray matter, total cerebral white matter, the supplied subcortical gray-matter aggregate, total cerebellum (left and right cortex plus white matter), and brainstem. All analyzed volumes were positive. Cohort-specific variable mappings are provided in the supplementary methods (Online Resource 1). These parts form an explicitly defined tissue composition, not an exhaustive decomposition of all intracranial contents.

Four orthonormal Helmert ILR coordinates represented the five-part vector. The omnibus test is invariant to rotation of the complete orthonormal basis, because all four coordinates span the same compositional subspace. Total analyzed tissue volume was log-transformed and modeled separately; estimated total intracranial volume (eTIV) was used in specified sensitivities. Additional nonlinear scale terms were evaluated in sensitivity models. These adjustments do not impose a specific white-matter-to-gray-matter scaling exponent.

$$b = \frac{1}{\sqrt{2}} ln(\frac{total\ cerebellum}{cerebral\ white\ matter})$$

Equivalently, b = ln(total cerebellum / cerebral white matter) / √2. An orthonormal basis was rotated so this was the first coordinate, with all three remaining coordinates retained. The focal balance and cognitive outcome were standardized within cohort. Its coefficient is the SD difference in the cognitive score per one-SD higher balance, conditional on age, sex, tissue scale and the remaining compositional coordinates.

## 2.6 Statistical models and uncertainty

Nested OLS models compared a baseline containing age, sex and log total analyzed tissue volume with a full model adding all four ILR coordinates. Added $R^2$ describes the increase in explained variance; partial $R^2$ is the reduction in residual sum of squares divided by the baseline residual sum of squares. The global comparison used a four-degree-of-freedom extra-sum-of-squares F test. HCP age bands were categorical. DLBS used a four-degree-of-freedom cubic B-spline of age-band midpoint, implemented as bs(age_mid, df=4, degree=3, include_intercept=False). AOMIC used linear age because its range was restricted to 19–26 years.

In discovery, all ten HCP pairwise log-ratio balances were examined and their nominal p values were adjusted using Holm's method. The selected total-cerebellum-to-cerebral-white-matter contrast was then tested unchanged in DLBS and AOMIC. Their cohort-specific tests use their own observations and covariance estimates; no HCP standard error enters either test. For the same sample and design matrix, changing only the OLS covariance estimator leaves fitted coefficients unchanged, but does not remove unmeasured confounding. AOMIC used fixed-sequence interpretation: the global test at $\alpha = .05$ preceded the targeted balance, assessed with a two-sided $\alpha = .05$ test and a required positive coefficient. Both were reported regardless of the sequence outcome. No alternative balance was selected using AOMIC results.

DLBS and AOMIC uncertainty checks used heteroskedasticity-robust HC3 covariance, a four-degree-of-freedom Wald F approximation for composition, and t-based focal intervals. Participant-pairs bootstraps used 2,000 resamples per cohort (seed 20261027), refitting PCA, score scaling and ILR standardizations. DLBS also refitted its age spline while retaining the original baseline domain composites, so its interval is conditional on that subtest calibration. Percentile intervals supplemented the primary tests. Separate numerical implementations checked estimates and covariance; these are computational checks, not independent human review.

Full-HCP standard errors were excluded from pooled inference. An exploratory synthesis summarized the DLBS and AOMIC focal coefficients using inverse-variance fixed-effect weighting and random effects with restricted maximum likelihood. Calculations used HC3 standard errors, with conventional OLS standard errors as a sensitivity. Because only two cohorts were available, normal-approximation random-effects intervals were accompanied by a modified Knapp–Hartung interval with one degree of freedom and variance inflation bounded below by one (Röver et al. 2015). Different cognitive batteries and within-cohort standardizations limit interpretation of this weighted summary as a common biological effect. Cohort-specific results remain primary.

## 2.7 Sensitivity and exploratory analyses

HCP and DLBS sensitivities examined eTIV as an alternative to or in addition to total tissue volume, one-factor or unit-weighted cognitive scores, nonlinear allometry, and structural quality (Table S2). HCP quality checks excluded public issue-code A or B flags. An additional sensitivity used the official S900 unrelated-subject list, selected for unrelatedness and multimodal completeness (Human Connectome Project n.d.-a, b). DLBS checks added education, excluded MMSE scores below 27, used categorical age bands, and adjusted standardized log1p surface-defect count. Quality proxies reduce some sources of morphometric bias but do not replace inspection of every image (Reuter et al. 2015; Rosen et al. 2018). Table S10 reports the focal coefficients under the three size-adjustment models in every cohort.

Exploratory analyses in all three cohorts examined raw-volume comparators, all ten pairwise balances, cognitive outcomes, and six-part cerebellar decompositions (Tables S3–S6). Tissue-class models separated cerebellar cortex and white matter and included a direct cortex-to-cerebellar-white-matter contrast; asymmetry models instead separated left and right total cerebellum. Each model retained all five coordinates of its six-part composition. Holm correction was applied within cohort to the ten pairwise contrasts, to the cognitive outcomes, and to the four cerebellar exploratory contrasts. DLBS also tested a linear age-by-balance interaction after adjustment for the nonlinear age main effect. Fig. 3 displays cohort-specific partial regressions after removing age, sex, log total tissue and the three other composition coordinates from both the standardized focal balance and cognitive score.

The frozen AOMIC sensitivity set evaluated native total cognition, quadratic age, alternative size adjustment, nonlinear allometry, surface defects, education, anatomical extremes and influence (Tables S8–S9; Fig. S1). Subset models retained primary PCA weights and predictor scales. Extremes were defined before testing by a five-scaled-median-absolute-deviation rule on log parts or log eTIV. Cook's distance > 4/N defined the influence diagnostic without redefining the primary sample. All nine sensitivity results are reported.

### 2.8 Ethics data governance and computational tools

The analysis used de-identified secondary data and involved no new participant contact. Original cohort ethics approvals, consent and data-use conditions are described in the Statements and Declarations. HCP participant-level data are not redistributed with this submission.

Analyses used Python with NumPy, pandas, SciPy, scikit-learn, statsmodels, patsy and openpyxl; versions and executable scripts are provided in Supplementary Code 1 (Online Resource 2). ChatGPT (OpenAI), including GPT-6 Astra Pro for this revision, assisted code development, computational checks, plotting, manuscript drafting and editing; Gemini (Google) provided editorial feedback. Estimates and figures were generated from source data by the supplied numerical algorithms and Matplotlib. Separate numerical implementations checked the principal calculations. AI tools are not authors.

## 3 Results

### 3.1 Cohort characteristics and cognitive scores

The analytical samples comprised 1,101 HCP-YA participants, 418 DLBS participants and 926 AOMIC participants (Table 1). All PC1 eigenvector weights were positive. PC1 explained 33.1% of variance across the ten HCP tests, 55.1% across five DLBS domain composites and 75.8% across three AOMIC domains. The AOMIC domain-to-PC1 correlations ranged from .850 to .895. These percentages depend on the number and aggregation of input measures and should not be interpreted as directly comparable cognitive reliability estimates. Table S1 distinguishes PCA weights from score correlations.

## Table 1. Analytical samples and descriptive characteristics

| Characteristic | HCP-YA | DLBS | AOMIC ID1000 |
|---|---|---|---|
| Analysis role | Discovery | Confirmation | Additional replication |
| Complete cases | 1,101 | 418 | 926 |
| Female / male | 596 / 505 | 260 / 158 | 481 / 445 |
| Age representation | Public bands: 22–25, 26–30, 31–35, 36+ | Band midpoints: 21–90 | Exact age: 19–26 |
| Mean age (SD), years | Not calculated from bands | 58.20 (18.30), midpoints | 22.85 (1.71) |
| Cognitive inputs | 10 test scores | 5 domain composites | 3 IST domains |
| PC1 variance explained | 33.1% | 55.1% | 75.8% |
| Total analyzed tissue, mean (SD), $cm^3$ | 1183.2 (122.8) | 1088.3 (116.1) | 1220.4 (118.5) |
| eTIV, mean (SD), $cm^3$ | 1580.5 (189.7) | 1539.4 (192.2) | 1645.8 (214.0) |
| Cortical gray matter, mean proportion (%) | 43.15 | 38.55 | 41.66 |
| Cerebral white matter, mean proportion (%) | 37.54 | 42.10 | 39.20 |
| Subcortical gray matter, mean proportion (%) | 5.17 | 5.16 | 5.06 |
| Total cerebellum, mean proportion (%) | 12.30 | 12.21 | 12.34 |
| Brainstem, mean proportion (%) | 1.85 | 1.98 | 1.75 |

Note. Sex categories follow the released variables. DLBS age values are modeled band midpoints, not exact ages; the published baseline cohort spans 21–89 years. Tissue proportions are means of participant-level fractions. eTIV, estimated total intracranial volume; IST, Intelligence Structure Test; PC1, first principal component. Descriptive differences also reflect cohort recruitment and processing differences.

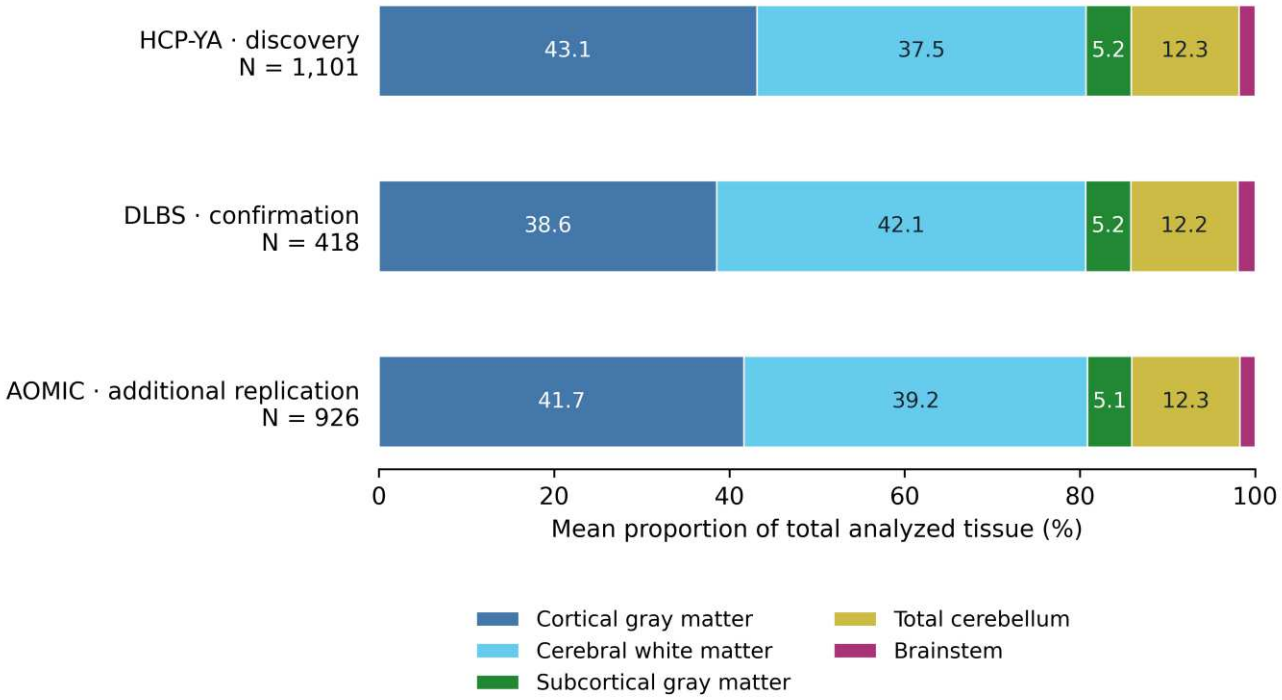



**Fig. 1 Cohorts and five-part tissue composition. Bars show mean within-participant proportions of cortical gray matter, cerebral white matter, subcortical gray matter, total cerebellum and brainstem. Cohorts are displayed in the actual analysis order: HCP discovery, DLBS confirmation and AOMIC additional replication. Proportions describe the analyzed tissue vector rather than all intracranial contents. Bars are descriptive cohort summaries; the association models additionally account for age, sex and log total analyzed tissue volume**

### 3.2 Global composition

In HCP-YA, adding the composition block increased $R^2$ from .1003 to .1371 ($\Delta R^2$ = .0368; partial $R^2$ = .0409). In DLBS, $R^2$ increased from .4657 to .4882 ($\Delta R^2$ = .0224; partial $R^2$ = .0420), with F(4,407) = 4.46, p = .00154. In AOMIC, $R^2$ increased from .0666 to .0792 ($\Delta R^2$ = .0126; partial $R^2$ = .0135), with F(4,918) = 3.14, p = .014. HC3 block tests supported the association in DLBS (p = .00277) and AOMIC (p = .017). The variance increment was smaller in AOMIC (Table 2; Fig. 2).

## Table 2. Global four-coordinate composition association

| Cohort | N | Baseline $R^2$ | Full $R^2$ | Added $R^2$ | Partial $R^2$ | Global p |
|---|---|---|---|---|---|---|
| HCP-YA | 1,101 | 0.1003 | 0.1371 | 0.0368 | 0.0409 | See note |
| DLBS | 418 | 0.4657 | 0.4882 | 0.0224 | 0.0420 | .00154 |
| AOMIC | 926 | 0.0666 | 0.0792 | 0.0126 | 0.0135 | .014 |

Note. Baseline models include age, sex and log total analyzed tissue volume. The full models add four ILR coordinates. Conventional tests: DLBS F(4,407) = 4.463; AOMIC F(4,918) = 3.144. Robust HC3 block p values are .00277 for DLBS and .0171 for AOMIC. HCP $R^2$ values describe discovery model fit. Added and partial $R^2$ are distinct quantities.

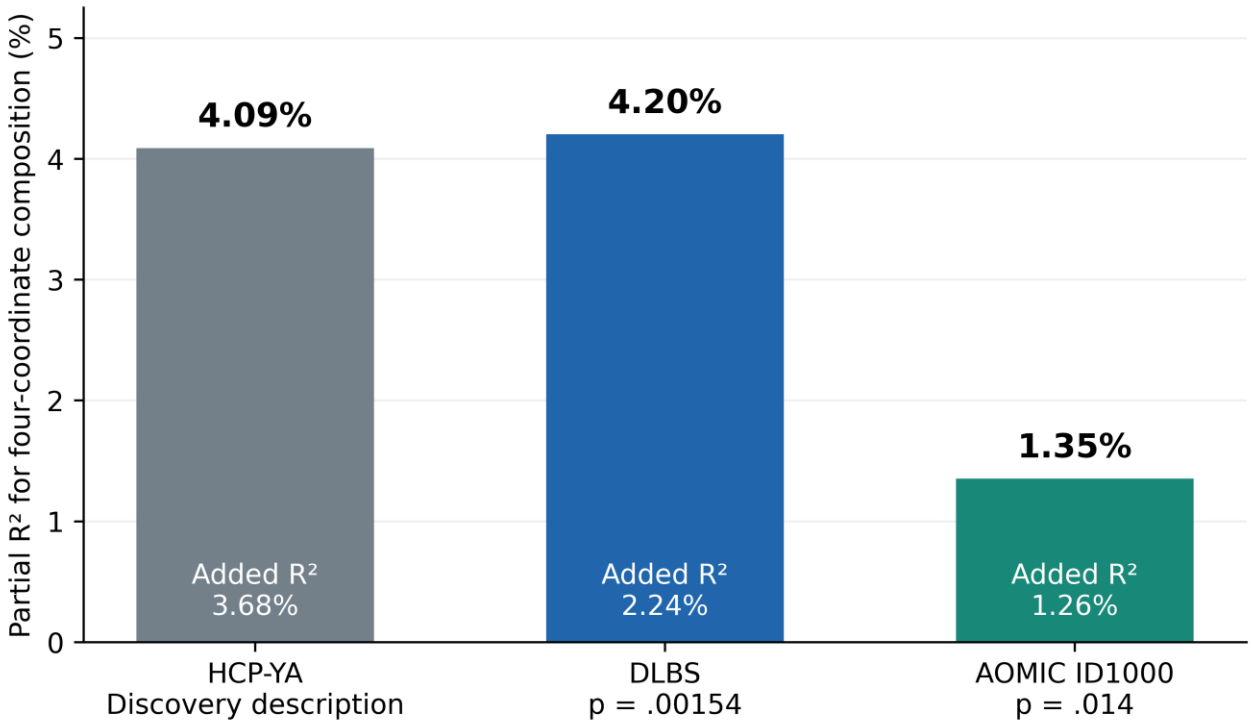



**Fig. 2 Global composition associations. The four-coordinate composition block is summarized by partial $R^2$ (bars) and added $R^2$ (annotations). HCP provides a descriptive discovery estimate. DLBS and AOMIC p values are conventional four-degree-of-freedom nested-model tests. Cohorts differ in age adjustment and cognitive measurement; equal effect magnitudes are not assumed**

### 3.3 Targeted cerebellum to cerebral white matter contrast

The focal HCP discovery coefficient was β = 0.204. It was positive in DLBS (β = 0.162, conventional 95% CI 0.082–0.243, p = $8.79 \times 10^{-5}$) and AOMIC (β = 0.097, conventional 95% CI 0.024–0.169, p = .0091). Both AOMIC tests met the specified global-then-focal sequence. DLBS HC3 uncertainty gave a 95% CI of 0.072–0.252 (p = .00043), and its bootstrap interval was 0.067–0.256. AOMIC HC3 uncertainty gave 0.024–0.170 (p = .0096), with a bootstrap interval of 0.025–0.165. All 2,000 resamples succeeded in each cohort. Table 3 presents conventional and robust estimates; Fig. 3 combines cohort-specific partial-regression plots with HC3 intervals.

## Table 3. Targeted cerebellum to cerebral white matter balance

| Cohort | N | β | OLS 95% CI | OLS p | HC3 95% CI | HC3 p |
|---|---|---|---|---|---|---|
| HCP-YA | 1,101 | 0.204 | — | — | — | — |
| DLBS | 418 | 0.162 | [0.082, 0.243] | $8.79 \times 10^{-5}$ | [0.072, 0.252] | .00043 |
| AOMIC | 926 | 0.097 | [0.024, 0.169] | .00906 | [0.024, 0.170] | .00965 |

Note. The balance is ln(total cerebellum/cerebral white matter)/√2. Coefficients adjust for age, sex, log total tissue volume and all three remaining orthogonal composition coordinates. β is standardized within cohort; intervals use residual-degrees-of-freedom t quantiles. HCP is presented as a discovery point estimate. Percentile bootstrap 95% intervals: DLBS [0.067, 0.256], AOMIC [0.025, 0.165], with 2,000 successful resamples each (Table S11).

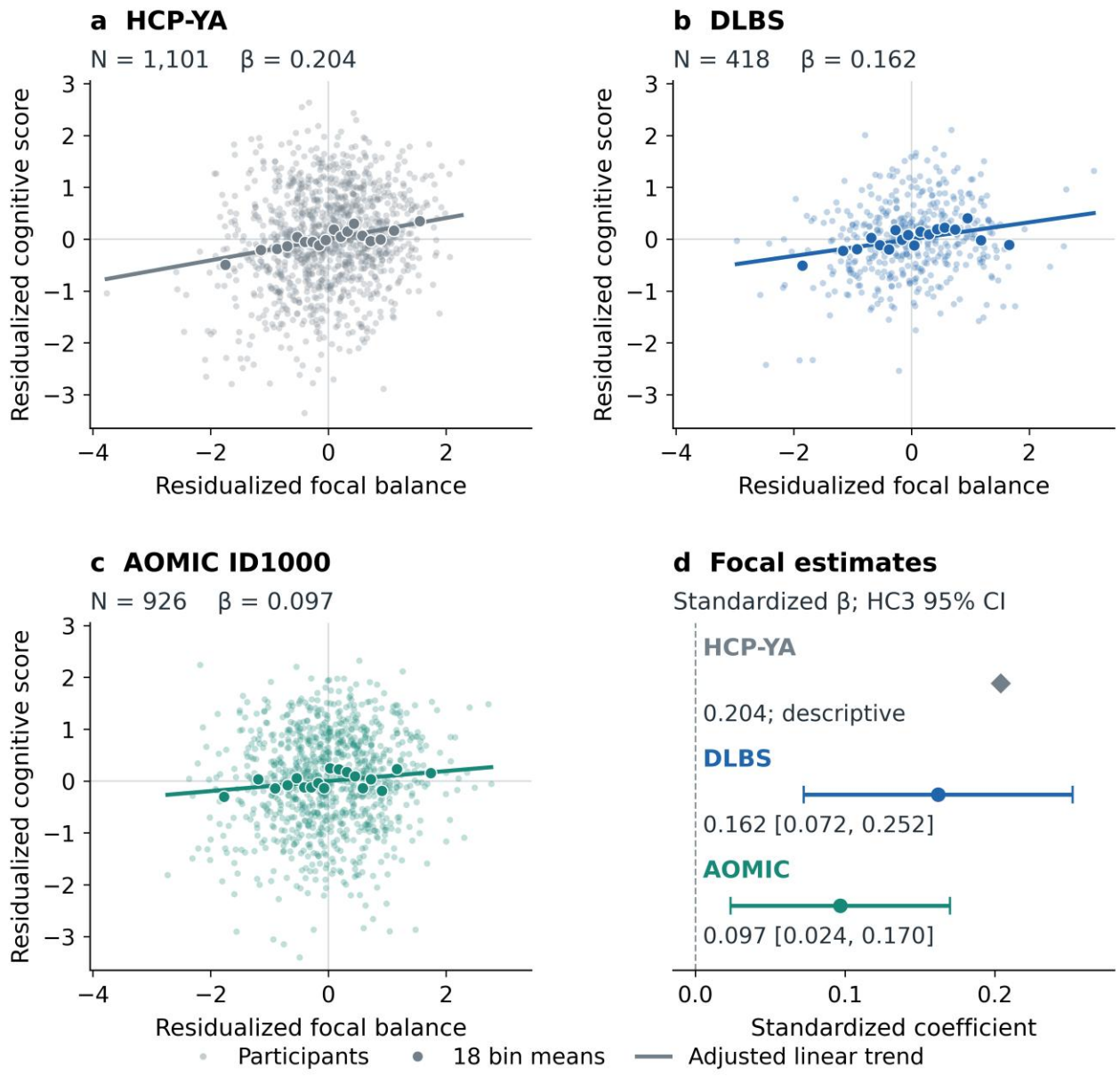



**Fig. 3 Cohort-specific partial regressions and targeted-balance estimates. Panels a–c plot all participants after residualizing the standardized cognitive score and focal balance against age, sex, log total analyzed tissue volume and the three remaining orthogonal composition coordinates. Lines show adjusted slopes; larger points show means in 18 equal-count bins. Residuals are not restandardized. Panel d gives the focal coefficients and HC3 95% confidence intervals for DLBS and AOMIC; HCP is shown as a descriptive point without an interval. Separate panels retain cohort-specific covariate structures and cognitive measures**

### 3.4 AOMIC sensitivity results

All p values in this paragraph use HC3 covariance. The AOMIC association persisted with the native IST total (β = 0.093; HC3 p = .014), quadratic age (β = 0.096; p = .010), nonlinear allometry (β = 0.098; p = .0092), surface-defect adjustment (β = 0.126; p = .0012), and educational categories (β = 0.114; p = .0010). Removing one anatomical extreme left β = 0.097 (p = .0095). The Cook's-distance diagnostic excluded 48 observations and gave β = 0.113 (p = .0006); it remains supplementary to the complete primary sample. Full conventional and robust results are retained in the supplement.

The alternative size adjustment materially changed the AOMIC result. Replacing log total tissue volume with log eTIV yielded β = 0.017 (HC3 95% CI −0.055 to 0.088, p = .648); the global conventional test was also nonsignificant (p = .078; HC3 p = .070). Including both log tissue volume and log eTIV preserved the association (β = 0.098, HC3 95% CI 0.026–0.171, p = .0081). The replication therefore supports the original total-tissue-conditional question, without establishing invariance to the choice of brain-size covariate.

### 3.5 Cross-cohort sensitivities and exploratory anatomical context

HCP structural-QC exclusions left N = 1,029 and a focal coefficient of 0.205. DLBS quality adjustment and expanded allometric models retained the composition association, and its age-by-balance interaction was not significant (p = .548). Under eTIV-only adjustment, the focal coefficient remained positive in HCP (β = 0.125; nominal $p = 7.64 \times 10^{-5}$) and DLBS (β = 0.108; HC3 95% CI 0.026–0.190, p = .0104), whereas it attenuated in AOMIC (Table S10). Thus, the AOMIC attenuation is not common to all three cohorts, but adjustment sensitivity remains a substantive qualification.

The reproducible official S900 sensitivity included 337 complete cases from the 339-person unrelated list. Partial $R^2$ was 1.16% (global p = .432), and the focal coefficient was 0.101 (conventional 95% CI −0.028 to 0.230, p = .125; HC3 p = .136; Table S7). This subset was selected for multimodal completeness as well as unrelatedness. Its attenuated estimate was imprecise.

All 18 cognitive test or domain coefficients were positive (Table S5). In AOMIC, the estimates were 0.099 for crystallized intelligence, 0.081 for fluid intelligence and 0.073 for memory; only crystallized intelligence retained statistical support after the three-domain Holm correction (Holm-adjusted HC3 p = .021). These tests do not demonstrate differences between domains. Cerebellar-cortex-to-cerebral-white-matter coefficients were positive in HCP (β = 0.219), DLBS (0.177) and AOMIC (0.105). AOMIC also showed a positive cerebellar-white-matter coefficient (0.109), while its direct cortex-to-cerebellar-white-matter contrast was small (0.019; HC3 p = .628). The direct contrast was positive in DLBS (0.137; HC3 p = .00345) and descriptively in HCP (0.097). Gross left–right asymmetry was associated with cognition in AOMIC (β = 0.090; HC3 p = .0064), but not in HCP or DLBS (Table S6). These findings do not establish a consistent tissue-class or asymmetry mechanism across cohorts.

### 3.6 Exploratory two-cohort synthesis

The DLBS–AOMIC synthesis included 1,344 participants (Table S12). Using HC3 standard errors, the inverse-variance fixed-effect summary was β = 0.123 (95% CI 0.066–0.180, $p = 2.09 \times 10^{-5}$); the REML random-effects normal-approximation summary was 0.124 (0.061–0.187, p = .00012). The modified Knapp–Hartung interval was −0.286 to 0.534 (p = .162). With k = 2 cohorts, this interval uses one degree of freedom and a 97.5th-percentile t critical value of 12.71, compared with the normal critical value of

1.96. Its width reflects limited precision for the mean association across populations. This random-effects interval includes zero; the positive individual cohort tests and fixed-effect summary answer different questions and do not remove that uncertainty.

# 4 Discussion

## 4.1 Principal findings

Relative allocation among five compartments was associated with cognition conditional on age, sex and total analyzed tissue volume. Positive global and targeted DLBS and AOMIC tests followed HCP discovery. AOMIC extended the result across another battery and pipeline, with a smaller global partial $R^2$ (1.35% versus 4.20% in DLBS) and focal coefficient (0.097 versus 0.162). The findings support the association's direction, without establishing a universal magnitude.

Thus, overall tissue scale does not exhaust the structural information associated with cognition. Relative configuration carries additional information among people with similar modeled covariates. These cross-sectional associations do not demonstrate causal tissue redistribution, substitution or optimal allocation.

## 4.2 Anatomical proportionality and scaling

The focal balance describes total cerebellar volume relative to cerebral white matter, conditional on the other composition coordinates and total analyzed tissue volume. The cortical-gray-matter-to-cerebral-white-matter balance was also positive in HCP, DLBS and AOMIC ($\beta$ = 0.150, 0.104 and 0.118; Table S4). The corresponding focal cerebellar coefficients were 0.204, 0.162 and 0.097, so their ordering was not identical across cohorts. Separate raw-volume comparators likewise gave negative conditional cerebral-white-matter coefficients in all three cohorts, despite positive marginal correlations with cognition (Table S3). These are conditional relative associations, not evidence that white matter is harmful or that either gray-matter compartment is absolutely enlarged.

Anatomical scaling provides a framework for interpreting this pattern. Zhang and Sejnowski (2000) derived a model relating cerebral white-matter volume to cortical gray-matter volume to the 4/3 power at fixed cortical thickness; the observed mammalian exponent was approximately 1.23. This geometry-based account links tissue proportions to the spatial requirements of cortical connectivity. It does not establish the same exponent among adults within these cohorts. Here, conditioning on the sum of five selected compartments asks whether their relative allocation is associated with cognition at a given analyzed tissue scale. The convergence of cortical and cerebellar balances therefore motivates a hypothesis about the relative volumes devoted to gray-matter-rich compartments and cerebral connections, rather than demonstrating neuronal efficiency or a causal trade-off. Neuron counts are distributed very differently from tissue mass (Azevedo et al. 2009), and these MRI volumes cannot measure neuronal number, axonal caliber, myelination or computational capacity.

Structural studies have linked cerebellar volume to cognition with effects depending on size adjustment (Andreasen et al. 1993; Paradiso et al. 1997; Hoogendam et al. 2014), while functional mapping links cerebellar regions to distributed association networks (Buckner et al. 2011). The present coarse volumes cannot identify those circuits. The tissue-class extension also does not support a universal cortex-specific account: both cerebellar components were positive relative to cerebral white matter in AOMIC and their

direct contrast was small. Dedicated cerebellar localization would help distinguish these anatomical possibilities (Diedrichsen et al. 2009).

### 4.3 Total tissue volume and intracranial volume answer different questions

Total analyzed tissue volume (T) sums the five modeled compartments; FreeSurfer eTIV is an atlas-scaling estimate of intracranial capacity (Buckner et al. 2004). They are related but not interchangeable. The identity $a \log(T) + c \log(eTIV) = (a + c) \log(eTIV) + a \log(T/eTIV)$ shows that a dual-size model can equivalently use intracranial capacity and the selected-tissue-to-eTIV ratio. This verified algebraic reparameterization is not an additional biological test. T/eTIV is not a complete parenchymal fraction because the five parts do not exhaust intracranial contents.

The AOMIC contrast became small and imprecise when eTIV replaced total tissue volume, but remained positive when both were included. The result therefore supports the original tissue-scale-conditional question while limiting claims of general independence from brain or head size. Bias in atlas-derived eTIV has been demonstrated in a validation sample (Klasson et al. 2018), but our analyses cannot establish whether measurement error, covariate correlations or biological differences explain the attenuation. CoDA does not remove confounding or determine the scientifically appropriate size covariate. The raw-volume comparisons (Table S3) reinforce the need to define the adjustment target; they do not show that compositional regression is universally superior for every morphometric question.

### 4.4 Strengths and limitations

Strengths include the low-dimensional anatomical representation, preservation of the original focal contrast across cohorts, independent cohort tests, complete reporting of the original AOMIC sensitivity set, and computational verification. Matching exploratory analyses across all three cohorts and robust uncertainty checks in both confirmation cohorts allow direct assessment of consistency and differences. The contribution builds on compositional neuroimaging (Genius et al. 2025) by focusing on cognition and major tissue compartments rather than disease-stage discrimination.

Full-sample HCP uncertainty remains unadjusted for family dependence, and the official unrelated-subject sensitivity was weaker and imprecise. DLBS and AOMIC supply independent tests of the selected contrast; they do not resolve unmeasured confounding in any cohort. Authorized family identifiers would permit a cluster-aware HCP analysis. The two-cohort synthesis also has limited information on between-population variation, as its wide modified Knapp–Hartung interval shows.

The cohorts also differ in cognitive measurement, age distributions, recruitment and MRI processing. AOMIC's cognitive PC1 uses three domain scores and is not psychometrically identical to the ten-test HCP or five-domain DLBS score. Its narrow young-adult age range limits inference about lifespan variation; the nonsignificant DLBS age interaction does not prove invariance across age. Cohort-specific FreeSurfer summaries were retained, and the study did not reprocess or independently inspect every raw scan. Public quality flags and surface-defect covariates address some measurement concerns but cannot eliminate them (Reuter et al. 2015; Rosen et al. 2018). Genetic unrelatedness was not independently established in AOMIC.

Finally, the cross-sectional design cannot distinguish developmental, genetic, vascular, aging-related or other influences. The composition omits some intracranial contents and uses broad anatomical classes. The exploratory cerebellar refinements and cognitive-domain analyses require targeted confirmation,

particularly where their patterns differ across cohorts. Neither the focal ratio nor the exploratory asymmetry findings establish a neural mechanism, causal tissue trade-off or intervention target.

### 4.5 Conclusion

A five-part macroanatomical composition and a previously selected total-cerebellum-to-cerebral-white-matter contrast were associated with broad cognitive ability in DLBS and AOMIC following HCP discovery. The AOMIC result was smaller and conditional on total analyzed tissue volume. Relative tissue proportionality adds an anatomical perspective on cognitive differences, with longitudinal and finer-grained studies needed to investigate its origins.

## References


Aitchison J (1986) The Statistical Analysis of Compositional Data. Chapman & Hall.

Andreasen NC, Flaum M, Swayze V II, O'Leary DS, Alliger R, Cohen G, Ehrhardt J, Yuh WTC (1993) Intelligence and brain structure in normal individuals. American Journal of Psychiatry 150:130–134. https://doi.org/10.1176/ajp.150.1.130

Azevedo FAC, Carvalho LRB, Grinberg LT, Farfel JM, Ferretti REL, Leite REP, Jacob Filho W, Lent R, Herculano-Houzel S (2009) Equal numbers of neuronal and nonneuronal cells make the human brain an isometrically scaled-up primate brain. Journal of Comparative Neurology 513:532–541. https://doi.org/10.1002/cne.21974

Buckner RL, Head D, Parker J, Fotenos AF, Marcus D, Morris JC, Snyder AZ (2004) A unified approach for morphometric and functional data analysis in young, old, and demented adults using automated atlas-based head size normalization: Reliability and validation against manual measurement of total intracranial volume. NeuroImage 23:724–738. https://doi.org/10.1016/j.neuroimage.2004.06.018

Buckner RL, Krienen FM, Castellanos A, Diaz JC, Yeo BTT (2011) The organization of the human cerebellum estimated by intrinsic functional connectivity. Journal of Neurophysiology 106:2322–2345. https://doi.org/10.1152/jn.00339.2011

Dale AM, Fischl B, Sereno MI (1999) Cortical surface-based analysis: I. Segmentation and surface reconstruction. NeuroImage 9:179–194. https://doi.org/10.1006/nimg.1998.0395

Deary IJ, Penke L, Johnson W (2010) The neuroscience of human intelligence differences. Nature Reviews Neuroscience 11:201–211. https://doi.org/10.1038/nrn2793

Diedrichsen J, Balsters JH, Flavell J, Cussans E, Ramnani N (2009) A probabilistic MR atlas of the human cerebellum. NeuroImage 46:39–46. https://doi.org/10.1016/j.neuroimage.2009.01.045

Dubois J, Galdi P, Paul LK, Adolphs R (2018) A distributed brain network predicts general intelligence from resting-state human neuroimaging data. Philosophical Transactions of the Royal Society B: Biological Sciences 373:20170284. https://doi.org/10.1098/rstb.2017.0284

Egozcue JJ, Pawlowsky-Glahn V, Mateu-Figueras G, Barceló-Vidal C (2003) Isometric logratio transformations for compositional data analysis. Mathematical Geology 35:279–300. https://doi.org/10.1023/A:1023818214614

Fischl B (2012) FreeSurfer. NeuroImage 62:774–781. https://doi.org/10.1016/j.neuroimage.2012.01.021

Fischl B, Salat DH, Busa E, Albert M, Dieterich M, Haselgrove C, van der Kouwe A, Killiany R, Kennedy D, Klaveness S, Montillo A, Makris N, Rosen B, Dale AM (2002) Whole brain segmentation: Automated labeling of neuroanatomical structures in the human brain. Neuron 33:341–355. https://doi.org/10.1016/S0896-6273(02)00569-X

Genius P, Calle ML, Rodríguez-Fernández B, Minguillon C, Cacciaglia R, Garrido-Martin D, Esteller M, Navarro A, Gispert JD, Vilor-Tejedor N, Alzheimer's Disease Neuroimaging Initiative and ALFA Study (2025) Compositional brain scores capture Alzheimer's disease-specific structural brain patterns along the disease continuum. Alzheimer's & Dementia 21:e14490. https://doi.org/10.1002/alz.14490

Hilger K, Winter NR, Leenings R, Sassenhagen J, Hahn T, Basten U, Fiebach CJ (2020) Predicting intelligence from brain gray matter volume. Brain Structure and Function 225:2111–2129. https://doi.org/10.1007/s00429-020-02113-7

Hoogendam YY, van der Geest JN, Niessen WJ, van der Lugt A, Hofman A, Vernooij MW, Ikram MA (2014) The role of cerebellar volume in cognition in the general elderly population. Alzheimer Disease & Associated Disorders 28:352–357. https://doi.org/10.1097/WAD.0000000000000024

Human Connectome Project (2025) HCP-Young Adult 2025 Release. https://www.humanconnectome.org/study/hcp-young-adult/document/hcp-young-adult-2025-release. Accessed 27 October 2026

Human Connectome Project (n.d.-a) HCP-YA Subjects with Identified Quality Control Issues (QC_Issue measure codes explained). HCP Public Pages. https://wiki.humanconnectome.org/docs/HCP%20Subjects%20with%20Identified%20Quality%20Control%20Issues%20%28QC_Issue%20measure%20codes%20explained%29.html. Accessed 27 October 2026

Human Connectome Project (n.d.-b) S900 Unrelated Subjects CSV. HCP Public Pages. https://wiki.humanconnectome.org/docs/S900%20Unrelated%20Subjects%20CSV.html. Accessed 27 October 2026

Jung RE, Haier RJ (2007) The parieto-frontal integration theory (P-FIT) of intelligence: Converging neuroimaging evidence. Behavioral and Brain Sciences 30:135–154. https://doi.org/10.1017/S0140525X07001185

Klasson N, Olsson E, Eckerström C, Malmgren H, Wallin A (2018) Estimated intracranial volume from FreeSurfer is biased by total brain volume. European Radiology Experimental 2:24. https://doi.org/10.1186/s41747-018-0055-4

Paradiso S, Andreasen NC, O'Leary DS, Arndt S, Robinson RG (1997) Cerebellar size and cognition: Correlations with IQ, verbal memory and motor dexterity. Neuropsychiatry, Neuropsychology, and Behavioral Neurology 10:1–8.

Park DC, Hennessee JP, Smith ET, Chan MY, Chen X, Dakanali M, Farrell ME, Liu P, Lu H, Rofsky N, Sun X, Tamminga C, Moore W, Kennedy KM, Rodrigue KM, Wig GS (2025) The Dallas Lifespan Brain Study: A comprehensive adult lifespan data set of brain and cognitive aging. Scientific Data 12:846. https://doi.org/10.1038/s41597-025-04847-7

Pietschnig J, Penke L, Wicherts JM, Zeiler M, Voracek M (2015) Meta-analysis of associations between human brain volume and intelligence differences: How strong are they and what do they mean? Neuroscience & Biobehavioral Reviews 57:411–432. https://doi.org/10.1016/j.neubiorev.2015.09.017

Reuter M, Tisdall MD, Qureshi A, Buckner RL, van der Kouwe AJW, Fischl B (2015) Head motion during MRI acquisition reduces gray matter volume and thickness estimates. NeuroImage 107:107–115. https://doi.org/10.1016/j.neuroimage.2014.12.006

Rosen AFG, Roalf DR, Ruparel K, Blake J, Seelaus K, Villa LP, Ciric R, Cook PA, Davatzikos C, Elliott MA, Garcia de La Garza A, Gennatas ED, Quarmley M, Schmitt JE, Shinohara RT, Tisdall MD, Craddock RC, Gur RE, Gur RC, Satterthwaite TD (2018) Quantitative assessment of structural image quality. NeuroImage 169:407–418. https://doi.org/10.1016/j.neuroimage.2017.12.059

Röver C, Knapp G, Friede T (2015) Hartung-Knapp-Sidik-Jonkman approach and its modification for random-effects meta-analysis with few studies. BMC Medical Research Methodology 15:99. https://doi.org/10.1186/s12874-015-0091-1

Snoek L, van der Miesen MM, Beemsterboer T, van der Leij A, Eigenhuis A, Scholte HS (2021) The Amsterdam Open MRI Collection, a set of multimodal MRI datasets for individual difference analyses. Scientific Data 8:85. https://doi.org/10.1038/s41597-021-00870-6

Van Essen DC, Smith SM, Barch DM, Behrens TEJ, Yacoub E, Ugurbil K, WU-Minn HCP Consortium (2013) The WU-Minn Human Connectome Project: An overview. NeuroImage 80:62–79. https://doi.org/10.1016/j.neuroimage.2013.05.041

Wilcox RR, Hemmatian B, Varshney LR, Barbey AK (2026) The network architecture of general intelligence in the human connectome. Nature Communications 17:2027. https://doi.org/10.1038/s41467-026-68698-5

Zhang K, Sejnowski TJ (2000) A universal scaling law between gray matter and white matter of cerebral cortex. Proceedings of the National Academy of Sciences of the United States of America 97:5621–5626. https://doi.org/10.1073/pnas.090504197

## Statements and Declarations

### Funding

No specific external funding was received for the present secondary analysis.

### Competing interests

The author declares no competing interests.

### Ethics approval and consent to participate

The original HCP, DLBS and AOMIC protocols obtained ethics approval and informed consent, as reported in their cohort publications (Van Essen et al. 2013; Park et al. 2025; Snoek et al. 2021). The present study analyzed de-identified secondary data and involved no new recruitment, intervention or participant contact. HCP data were used under the applicable data-use terms; DLBS and AOMIC were accessed through their public OpenNeuro releases.

### Consent for publication

Not applicable to this report of de-identified secondary analyses; no identifiable participant details or images are presented.

### Data availability

HCP Young Adult data are available through the Human Connectome Project and ConnectomeDB under applicable data-use terms (https://www.humanconnectome.org/study/hcp-young-adult). DLBS data are available as OpenNeuro ds004856 v1.3.0 (https://doi.org/10.18112/openneuro.ds004856.v1.3.0); AOMIC ID1000 data are available as ds003097 v1.2.1 (https://doi.org/10.18112/openneuro.ds003097.v1.2.1). Source manifests and checksums accompany the code. HCP participant-level data are not redistributed; the AOMIC analysis subset follows its CC0 source release.

### Code availability

Supplementary Code 1 (Online Resource 2) contains executable analysis pipelines, the original AOMIC specification, source manifests, aggregate outputs and numerical verification. It includes the S900 sensitivity, exploratory extensions and two-cohort synthesis, with input retrieval and execution instructions. Restricted HCP family information is not included.

### Author contributions

Baptiste Dumoulin: Conceptualization, Methodology, Software, Formal analysis, Investigation, Data curation, Visualization, Writing – original draft, Writing – review and editing. AI assistance is described in Methods.

## Supplementary Files

This is a list of supplementary files associated with this preprint. Click to download.

- ESM1corrected.pdf
- ESM2.zip